

SADP: Subgoal-Aware Diffusion Policy for Explainable Robots Learned from Foundation Model Generated Demonstrations

Site Hu¹ and Takato Horii¹

Abstract—Explainable robots require not only successful task execution but also the ability to expose internal decision-making process in a user-friendly manner. However, most imitation learning methods are trained solely on task-level demonstrations, without explicitly modeling subgoal structure or execution progress. This limitation is further exacerbated by the scarcity of subgoal-level supervision in standard robot learning datasets, which restricts the development of robots that can convey the subtasks they are executing during long-horizon manipulation. To address this issue, this paper proposes Subgoal-Aware Diffusion Policy (SADP), a framework that leverages foundation models to autonomously generate subgoal-annotated demonstrations and trains diffusion policies on these datasets. SADP structures policy execution around human-interpretable subgoals by conditioning action generation on both task-level and subgoal-level descriptions. A lightweight auxiliary head further predicts subgoal completion states, allowing the robot to expose its current execution stage and monitor subgoal progression. Experiments in RLBench simulations and real-world evaluations on a UR5e robot demonstrate that SADP achieves higher task success rates than strong task-conditioned diffusion baselines, while providing subgoal-level execution signals for monitoring progress and diagnosing failures. These results highlight that built-in, rather than post-hoc, interpretability can coexist with high task performance.

I. INTRODUCTION

Autonomous robots are being deployed across an increasing range of domains as capable partners for humans. In these settings, robots are expected not only to accomplish tasks reliably, but also to do so transparently. Such transparency is a key prerequisite for fostering trust in human-robot interaction (HRI) [1], and becomes especially important in long-horizon manipulation tasks. These tasks typically unfold as a sequence of intermediate subgoals, such as grasping, transporting, and placing objects [2]. While humans naturally reason about and monitor progress at the subgoal level for these tasks, most learning-based methods for robots lack explicit representations of subgoals [3]. These policies typically operate at the task level, directly mapping observations and goals to low-level actions without explicitly modeling subgoal structure or execution progress. As a result, these policies behave as black boxes during execution, limiting their transparency and interpretability.

While subgoal decomposition has been extensively studied in hierarchical reinforcement learning (HRL) for long-horizon tasks, the subgoals in HRL are typically learned as latent representations or option-level abstractions that improve exploration efficiency, temporal abstraction, and scalability [4]. In parallel, much of explainable artificial intelligence (XAI) research in robotics has focused on post-hoc explanations that

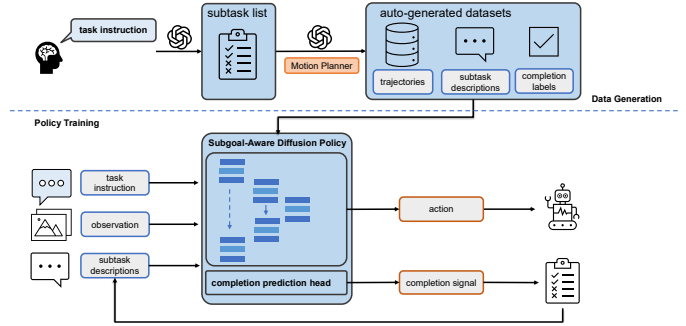


Fig. 1. Overview of the SADP. SADP autonomously collects demonstrations paired with structured subgoal descriptions and completion signals to train a subgoal-aware diffusion policy with a completion prediction head.

are generated after decisions are made [5]. Such explanations are decoupled from action generation and may not faithfully reflect the policy’s actual execution process. Therefore, a key gap remains: how to construct policies that are interpretable by design at the subgoal level, using subgoals that humans can naturally understand and interact with, without sacrificing the task performance of state-of-the-art black-box policies.

This gap is further amplified by commonly used robot learning datasets, which typically provide only task-level descriptions and lack explicit supervision of subgoals or execution progress. Although subgoal-aware learning becomes feasible when such annotations are available, collecting reliable subgoal labels for long-horizon, open-ended manipulation tasks is ambiguous and costly. Foundation models offer a promising alternative by generating structured task decompositions and synthesizing demonstrations from high-level instructions. Existing studies have mainly used foundation models for high-level planning [6], or for generating demonstrations to train task-level policies [7], [8]. However, these methods still treat the learned policy primarily as a task-level controller, without explicitly integrating human-interpretable subgoal structure into action generation or execution monitoring.

To bridge this gap, we propose **SADP** (Subgoal-Aware Diffusion Policy), a novel framework for robot manipulation. As illustrated in Fig. 1, SADP leverages foundation models to decompose a task instruction into an ordered subgoal list, and executes these subgoals sequentially using an LLM-generated motion planner. Crucially, the generated subgoals are expressed as natural-language descriptions, which serve as human-interpretable execution units that users can readily understand and use to monitor the robot’s progress. Through this process, SADP autonomously generates demonstrations paired with structured subgoal descriptions and completion signals, eliminating the need for manual subgoal annotation. Using this

¹Department of Systems Innovation, Graduate School of Engineering Science, Osaka University, Osaka, Japan

enriched dataset, SADP learns a diffusion-based policy that conditions action generation on both task-level instructions and subgoal descriptions, and includes a completion prediction head to estimate subgoal execution status. Consequently, at inference time, the policy can explicitly expose its current subgoal, providing subgoal-level execution transparency while preserving strong low-level control performance.

Our contributions can be summarized as follows:

- We propose SADP, an interpretable-by-design diffusion policy framework that uses foundation models to automatically generate demonstrations with human-interpretable natural-language subgoals and completion signals, eliminating manual subgoal annotation.
- We introduce a subgoal-aware diffusion policy that conditions action generation on both task-level instructions and current subgoal descriptions, and jointly predicts subgoal completion states to expose execution progress at the subgoal level.
- We evaluate SADP on six simulated tasks in RL Bench [9] and three real-world tasks, showing that explicit subgoal structure improves long-horizon manipulation performance while enabling progress monitoring and failure diagnosis through subgoal-level signals.

II. RELATED WORKS

A. Explainable Autonomous Robots for Long-Horizon Tasks

A central distinction in explainable AI research is between post-hoc explanation methods, which generate explanations after a black-box model has produced its output, and interpretable-by-design models, whose internal structure is itself meaningful to humans [10]. Post-hoc methods, such as feature attribution, rationales, and counterfactual explanations, are widely used because they can be applied to pretrained models [5], [11]. However, they suffer from a fundamental limitation: the explanation is decoupled from the actual decision process and may not faithfully reflect it. Interpretable-by-design models avoid this faithfulness issue, but in robot manipulation, existing interpretable structures often rely on hand-crafted task hierarchies, symbolic planners, or behavior trees, which may lack the expressiveness of modern learned policies. SADP addresses this gap by integrating human-interpretable subgoal structure directly into a diffusion policy.

Explainability is widely regarded as a prerequisite for trustworthy HRI, especially in long-horizon tasks in which robots serve as collaborative partners to humans [12], [13]. Research on explainable autonomous robots (XARs) has investigated how robots can convey their behavior and decision-making process in human-interpretable forms [14], [15], [16], [17]. However, many existing systems treat explanation as an auxiliary component decoupled from action generation and emphasize post-hoc explanations generated after decisions have been made or actions executed [5], [10], [11]. While post-hoc explanations can improve user comprehension, they may not faithfully reflect the decision-making process that actually drives execution, which is particularly problematic in long-horizon tasks.

Long-horizon manipulation tasks can typically be decomposed into a temporally extended sequence of subtasks [2]. HRL leverages this structure by introducing high-level subgoals and low-level policies, improving task-level performance through better exploration, credit assignment, and temporal abstraction in continuous long-horizon control [18], [19], [20]. However, the subgoals in HRL are typically learned latent representations whose semantics are not constrained to align with human-interpretable concepts [4]. SeqVLA [21] takes a step toward making progress explicit by introducing subtask completion detection, but it requires collecting subtask-level demonstrations and manually annotating completion signals. In contrast, SADP uses natural-language subgoals generated by foundation models, ensuring that the policy’s structure is interpretable from the outset. Our method further leverages foundation models to automatically generate demonstrations with structured subgoal descriptions and completion signals, eliminating the need for manual annotation. Moreover, by tightly coupling subgoal awareness with action generation, our approach yields execution signals that are directly associated with the robot’s behavior.

B. Diffusion Policies for Robot Manipulation

Diffusion policies have recently emerged as effective generative models for robot manipulation, casting action generation as conditional denoising and naturally capturing complex, multi-modal action distributions [22]. Building on this paradigm, prior work has improved diffusion policies through richer representations and conditioning mechanisms, yielding better performance and stronger multi-task instruction following across diverse manipulation tasks [8], [23], [24]. These methods typically condition on observations and task instructions, but they do not explicitly represent subgoal-aware structure; consequently, execution progress remains implicit in the policy dynamics. In contrast, our approach augments diffusion policies with explicit subgoal-conditioning and a completion prediction mechanism, enabling robust long-horizon task execution and transparent behavior.

C. Foundation Models for Robot Manipulation

Foundation models, including large language models (LLMs) and vision-language models (VLMs), have enabled robot manipulation systems with improved language understanding, planning, and perception. Many approaches use LLMs as high-level planners that call predefined motion primitives or controllers [25], [26], [27], while VLM-based perception improves scene understanding and spatial grounding for language-conditioned manipulation [6], [28], [29], [30]. However, directly using large foundation models during execution can introduce instability and non-determinism in closed-loop robot control [31].

Foundation models have also been used to scale data collection by generating demonstrations for policy learning [7], [8], [32], [31]. Although these methods reduce manual data collection and improve task-level performance, the resulting policies are usually trained as task-level controllers and do not explicitly expose subgoal-level execution progress.

Vision-language-action (VLA) models offer an end-to-end alternative by internalizing language-action mappings within large pretrained architectures [33], [34], [35]. Hierarchical and chain-of-thought variants further improve long-horizon execution [21], [36]. Nevertheless, their intermediate execution states often remain opaque to users at runtime, and they typically require large backbones and substantial fine-tuning. In contrast, SADP uses foundation models mainly for perception and subgoal-annotated demonstration generation, and distills human-interpretable subgoal structure into a lightweight diffusion policy. By explicitly exposing subgoal completion states through a dedicated prediction head, SADP provides a complementary form of runtime transparency.

III. METHOD

In this work, we propose SADP, a Subgoal-Aware Diffusion Policy framework for interpretable long-horizon robot manipulation. SADP is designed around a simple principle: the units that humans use to understand long-horizon tasks, i.e., natural-language subgoals, should also structure policy execution. Concretely, SADP conditions action generation on human-interpretable subgoal descriptions and exposes the policy’s execution state through subgoal completion prediction.

As illustrated in Fig. 1, SADP consists of two components: (1) a foundation-model-driven data generation pipeline that generates demonstrations annotated with natural-language subgoals and completion signals, and (2) a subgoal-aware diffusion policy that jointly learns subgoal-conditioned action generation and subgoal completion prediction.

A. Subgoal-Annotated Demonstration Generation

A major challenge in learning explainable robot policies that can convey their current subgoal lies in the lack of subgoal-level supervision. Most existing robot learning datasets provide only task-level labels and sparse success signals, which are insufficient for representing intermediate execution progress or decision states. Yang et al. [21] address this issue by collecting demonstrations for each subtask separately and manually annotating subgoal completion states for every frame. While effective, such manual annotation requires substantial human effort and does not scale well to diverse long-horizon tasks.

To address this limitation, we generate subgoal-annotated demonstrations by extending the affordance-based automatic data collection framework proposed by Hu et al. [8]. In our framework, foundation models decompose each task into human-interpretable natural-language subgoals, which are not merely used as offline annotations but serve as the structural basis of the learned policy.

Following [8], we use LLMs to decompose a natural-language instruction into a sequence of subgoals. For each subgoal, LLMs and VLMs extract affordance information represented by target-object point clouds and voxel value maps, which are then used by an LLM-generated heuristic motion planner to sequentially execute the subgoals. During execution, each trajectory is segmented according to the generated subgoal sequence. The final frame of each subgoal segment is labeled as 0, indicating completion, while all preceding frames

are labeled as 1, indicating ongoing execution. In this way, each demonstration is automatically associated with natural-language subgoal descriptions and frame-level completion labels. Finally, LLMs and VLMs filter successful executions, and the resulting trajectories are collected as a labeled dataset for training SADP.

B. Subgoal-Aware Diffusion Policy with Completion Prediction Head

As shown in Fig 2, The diffusion policy conditions on affordance observations represented by point clouds of target objects, together with task and subgoal descriptions, which are jointly encoded as a global conditioning vector c .

Based on the collected dataset annotated with both task- and subgoal-level labels, SADP learns a diffusion-based robot manipulation policy [22] that explicitly integrates subgoal information into action generation. At each timestep k , the conditional diffusion policy predicts the noise $\epsilon_\theta(a_k, k, c)$ added to the action, and iteratively denoises a random Gaussian noise vector through the reverse diffusion process to obtain the desired clean action.

Specifically, we concatenate the robot proprioceptive history, the 3D feature representation of the target object point cloud encoded by a lightweight MLP encoder (DP3) [23], and the text embeddings of task and subgoal descriptions encoded by a CLIP B/32 text encoder [37], forming the composite conditioning vector c . This conditioning vector is incorporated into the denoising process via FiLM [38]. Starting from a random Gaussian noise vector $a_K \sim \mathcal{N}(0, I)$, the denoising network e_θ is iteratively applied for K steps to obtain the final action a_0 . At each timestep k , the reverse diffusion update is given by

$$a_{k-1} = \frac{1}{\sqrt{\alpha_k}} \left(a_k - \frac{1 - \alpha_k}{\sqrt{1 - \bar{\alpha}_k}} \epsilon_\theta(a_k, k, c) \right) + \sigma_k z, \quad (1)$$

where α_k denotes the noise schedule parameter at timestep k , $\bar{\alpha}_k = \prod_{i=1}^k \alpha_i$, σ_k is the noise scale, and $z \sim \mathcal{N}(0, I)$. The action prediction loss is defined as the mean squared error between the true noise ϵ and the predicted noise:

$$\mathcal{L}_{\text{action}} = \mathbb{E}_{a_0, \epsilon, k} \left[\|\epsilon - \epsilon_\theta(a_k, k, c)\|^2 \right]. \quad (2)$$

As illustrated in Fig. 2, SADP augments the standard conditional diffusion model with a lightweight subgoal completion prediction head. This head is implemented as a binary classifier that shares the same conditioning vector c with the diffusion policy and outputs a binary classification score indicating subgoal completion probability:

$$p = \sigma(W \cdot c + b), \quad (3)$$

where $\sigma(\cdot)$ denotes the sigmoid function. Since subgoal-incomplete states significantly outnumber subgoal-complete states, we adopt focal loss [39] for the completion prediction head in order to mitigate class imbalance:

$$\mathcal{L}_{\text{completion}} = -\beta(1-p)^\gamma y \log(p) - (1-\beta)p^\gamma (1-y) \log(1-p), \quad (4)$$

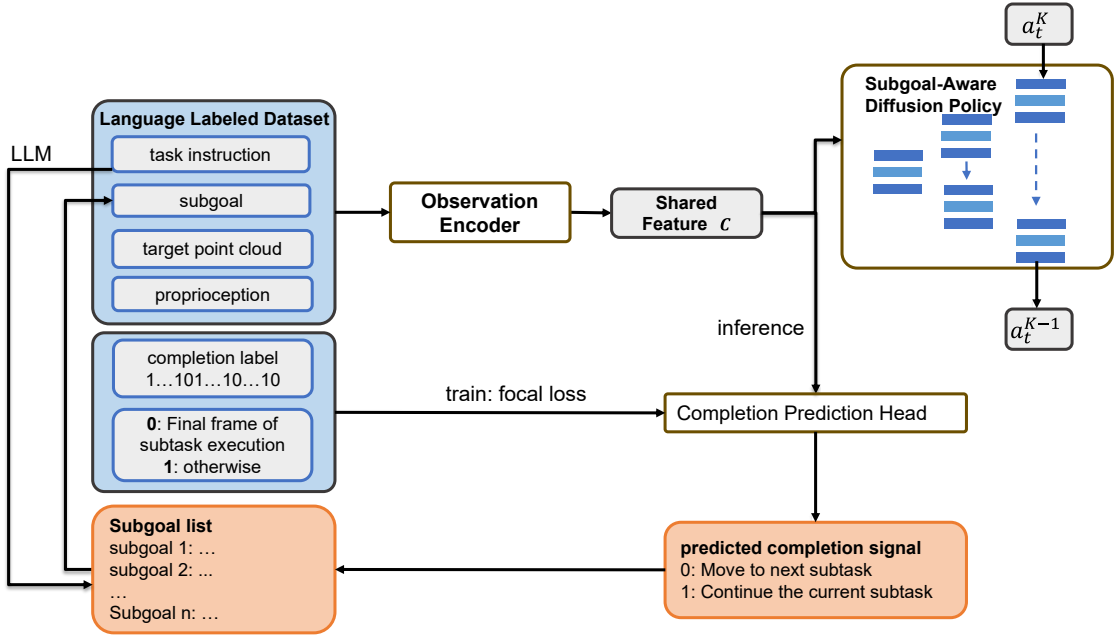


Fig. 2. Subgoal-aware diffusion policy with completion prediction head. The completion prediction head shares the same encoded observation features with the diffusion policy and outputs a binary classification score indicating subgoal completion probability.

where $y \in \{0, 1\}$ is the ground-truth completion label, and the focal loss hyperparameters β and γ are set to 0.25 and 2, respectively.

The overall training objective is given by

$$\mathcal{L}_{\text{total}} = \mathcal{L}_{\text{action}} + \lambda \mathcal{L}_{\text{completion}}, \quad (5)$$

where λ denotes the weight of the completion prediction loss and gradually increased from 0 to 0.1 during training to avoid destabilizing action learning in the early stage of training.

During training, we directly use the ground-truth subgoal labels provided in the dataset. During inference, we generate the subgoal sequence using LLMs in the same manner as in the data generation stage, and predict subgoal completion online. When the predicted completion probability p drops below a threshold τ , the current subtask is deemed completed and a completion signal is issued. This predicted completion signal triggers transitions to subsequent subgoals in the sequence, enabling structured long-horizon task execution. If the threshold τ is set too low, the policy struggles to trigger the completion signal, whereas an excessively high threshold may cause premature termination of the current subtask. We empirically set the threshold to 0.2 to balance these two effects.

IV. EXPERIMENTS

We evaluate SADP in both simulation and real-world environments to assess its effectiveness in long-horizon manipulation tasks. Our experiments are designed to answer the following questions:

- 1) Does integrating human-interpretable subgoal structure into a diffusion policy match or improve task-level performance in long-horizon manipulation tasks?

- 2) Are the subgoal-level signals produced by SADP temporally coherent and aligned with the policy’s execution progress, including in failure cases?
- 3) Does providing correct subgoal information improve long-horizon manipulation performance?

A. Experiment Setup

1) *Environments*: In our simulation study, we consider a set of long-horizon manipulation tasks from RL-Bench [9], a widely used benchmark for learning from demonstrations. These tasks require the sequential execution of multiple subgoals, posing significant challenges for long-horizon decision-making and making them particularly suitable for evaluating subgoal-aware policies. We evaluate SADP on six representative tasks, illustrated in Fig. 3. Their typical temporal structures are summarized as follows:

- 1) **PutRubbishInBin**: A pick-and-place task involving grasping the rubbish, moving through an intermediate pose, reaching above the bin, and releasing it.
- 2) **SlideBlockToTarget**: A pushing task involving repeated repositioning, and pushing the block toward the target zone.
- 3) **MeatOffGrill**: A pick-and-place task involving grasping the target meat, moving through an intermediate pose, reaching above the target area, and releasing it.
- 4) **OpenDrawer**: A drawer-interaction task involving gripper alignment, handle grasping, drawer pulling, and handle release.
- 5) **CloseDrawer**: A drawer-interaction task involving gripper alignment, handle contact, and pushing the drawer closed.
- 6) **PutItemInDrawer**: A longer multi-stage task combining drawer opening and object placement, involving handle

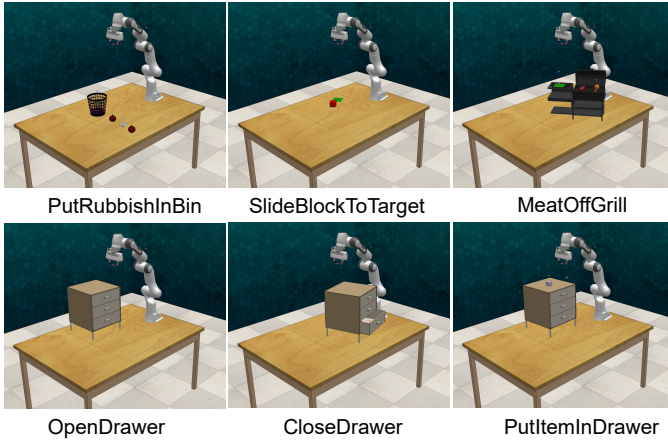


Fig. 3. Six tasks in simulation experiment. The tasks cover different temporal structures, ranging from pick-and-place to drawer interaction tasks.

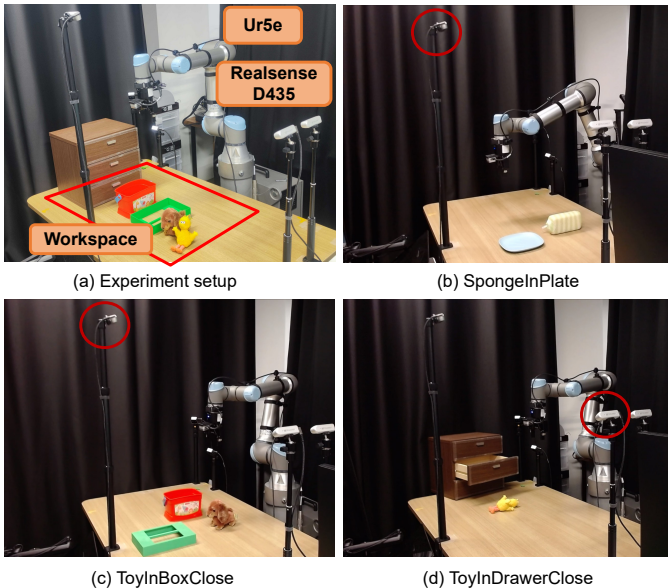


Fig. 4. Real-world experiment setup. The red circles indicate the RGB-D camera used in each task. The tasks range from pick-and-place to multi-stage manipulation involving object placement followed by box or drawer closing.

manipulation, object grasping, moving above the drawer, and releasing the object inside.

We also validate SADP on real-world manipulation tasks using a UR5e robotic arm equipped with a RealSense D435 camera for RGB-D image capture. The evaluation includes three tasks, as illustrated in Fig. 4:

- 1) **SpongeInPlate**: A pick-and-place task involving grasping the sponge, moving through an intermediate pose, reaching above the plate, and releasing it.
- 2) **ToyInBoxClose**: A longer task involving placing the toy dog into the box and then closing the lid.
- 3) **ToyInDrawerClose**: A longer task involving placing the toy dog into an open drawer and then closing the drawer.

2) *Baselines*: We compare SADP against two baselines trained on the same auto-collected datasets: a task-conditioned variant of point-cloud-based diffusion policy DP3 [23] and an

affordance-based diffusion policy TARAD [8]. These baselines condition action generation only on observations and task descriptions, without subgoal-aware structures.

3) *Dataset Construction*: We follow the affordance-based automatic data collection framework proposed in [8]. Specifically, we use LLMs to decompose natural language instructions into high-level task plans consisting of a sequence of subgoals. For example, the `PutRubbishInBin` task is decomposed into a sequence of subgoals: (1) grasping the rubbish, (2) reset to default position, (3) moving it above the bin, and (4) opening the gripper. Each subgoal is then executed by an affordance-driven heuristic motion planner. In simulation, affordance information is obtained directly from oracle object masks. In real-world settings, affordances are inferred from RGB-D observations using multi-modal VLM GPT-4o [40], the open-vocabulary object detector GroundingDINO [28], and the mask tracking framework Segment Anything 2 [29]. This pipeline enables the automatic execution of each subgoal and allows natural segmentation of collected long-horizon, task-level demonstrations into multiple subtask-level demonstrations for training SADP.

For each subtask-level demonstration, the final frame is labeled as 0, corresponding to the last action that completes the current subgoal, while all preceding frames are labeled as 1, indicating actions executed during subgoal progression. Accordingly, the label sequence of each task-level demonstration follows a pattern of the form $1 \dots 1 0 1 \dots 1 0 \dots 1 0$, where 1 denotes the execution phase and 0 denotes subgoal completion. The entire data collection process is fully driven by the LLM and requires no manual annotation.

We collected 30 demonstrations for each task. Task-level demonstrations are used to train baseline methods, whereas subtask-level demonstrations are used to train SADP.

4) *Evaluation Metric*: For simulation experiments, we trained each task for 2000 epochs using three random seeds. For each seed, we evaluated 20 episodes every 200 epochs and computed the average of the top three success rates. We report the mean and standard deviation of the success rates across the three seeds. For real-world experiments, we trained for 2000 epochs and evaluated the final checkpoint over 30 episodes.

B. Results

1) *Simulation Results*: Table I reports the task success rates in simulation. SADP consistently outperforms the point-cloud-based task-conditioned diffusion policy baseline DP3 across all six tasks, and achieves slightly better performance than the affordance-based diffusion policy baseline TARAD. These results indicate that integrating human-interpretable subgoal structure into diffusion policies can improve task-level performance in long-horizon manipulation, rather than sacrificing performance for transparency.

Compared with task-conditioned baselines, SADP structures execution around the current subgoal and updates the active subgoal according to the predicted completion state. This design helps reduce premature progression to subsequent stages when prerequisite subgoals remain incomplete, which is particularly important in tasks with sequential dependencies.

TABLE I
TASK SUCCESS RATES (%) OF SADP AND BASELINE METHODS ON SIX SIMULATED LONG-HORIZON MANIPULATION TASKS.

Model	PutRubbish InBin	SlideBlock ToTarget	MeatOff Grill	Open Drawer	Close Drawer	PutItem InDrawer	Average
DP3 [23]	77.8 ± 3.47	66.1 ± 5.85	51.1 ± 4.19	55.0 ± 5.00	74.4 ± 6.94	46.1 ± 2.55	61.8
TARAD [8]	88.9 ± 3.47	85.0 ± 2.89	73.3 ± 3.33	78.3 ± 4.41	92.8 ± 5.36	73.9 ± 6.31	82.0
Ours	92.2 ± 2.55	85.6 ± 7.52	78.9 ± 7.88	75.0 ± 5.00	93.9 ± 4.82	71.1 ± 5.36	82.8

TABLE II
TASK SUCCESS RATES (%) OF SADP AND BASELINE METHODS ON THREE REAL-WORLD LONG-HORIZON MANIPULATION TASKS.

Model	SpongeInPlate	ToyInBoxClose	ToyInDrawerClose
DP3	83.3	40.0	46.7
TARAD	96.7	56.7	76.7
Ours	90.0	73.3	86.7

2) *Real-World results:* Table II summarizes the success rates of SADP and the baselines in real-world experiments. SADP remains effective in real-world settings. Although TARAD slightly outperforms SADP on the relatively short SpongeInPlate task, where subgoal-aware execution is less critical, SADP substantially outperforms both baselines on the two longer-horizon drawer-related tasks.

These results suggest that subgoal-aware conditioning and explicit completion prediction are especially beneficial for real-world manipulation tasks involving multiple sequential interaction stages. By maintaining execution consistency across subgoals, SADP reduces failure accumulation and improves reliability in long-horizon execution.

C. Subgoal-Level Execution Transparency

We qualitatively analyze the subgoal-level execution signals produced by SADP during long-horizon manipulation. Fig. 5 visualizes the predicted subgoal completion scores for a representative successful trajectory of the **ItemInDrawer** task, while Fig. 6 shows a representative failed trajectory of the same task. The completion score represents the predicted completion state of the current subgoal, where lower scores indicate higher confidence that the current subgoal has been completed.

In the successful trajectory shown in Fig. 5, the active subgoal changes sequentially as the robot progresses through the task. The robot first aligns the gripper with the drawer handle, grasps the handle, opens the drawer, releases the handle, resets the arm, grasps the target item, moves it above the drawer, and finally opens the gripper to drop the item. The predicted completion scores are temporally correlated with these execution stages: the score remains relatively high while a subgoal is being executed and decreases when the robot reaches the corresponding intermediate objective. This pattern suggests that the completion predictor captures meaningful temporal boundaries between subgoals.

The failed trajectory in Fig. 6 further illustrates the diagnostic value of the exposed subgoal-level signal. In this

example, the robot successfully proceeds through the initial alignment and handle-grasping stages. However, during the drawer-opening subgoal, the gripper disengages from the drawer handle. Correspondingly, completion of this subgoal is not detected, and the active subgoal remains fixed instead of advancing to the subsequent item-grasping stage. The failure can therefore be localized to the drawer-opening stage from the exposed execution state.

These results show that the subgoal completion predictions provide temporally structured execution cues aligned with the visible progress of long-horizon manipulation. By exposing the active subgoal and its predicted completion state, SADP allows the execution process to be inspected at the subgoal level, improving the transparency of policy behavior.

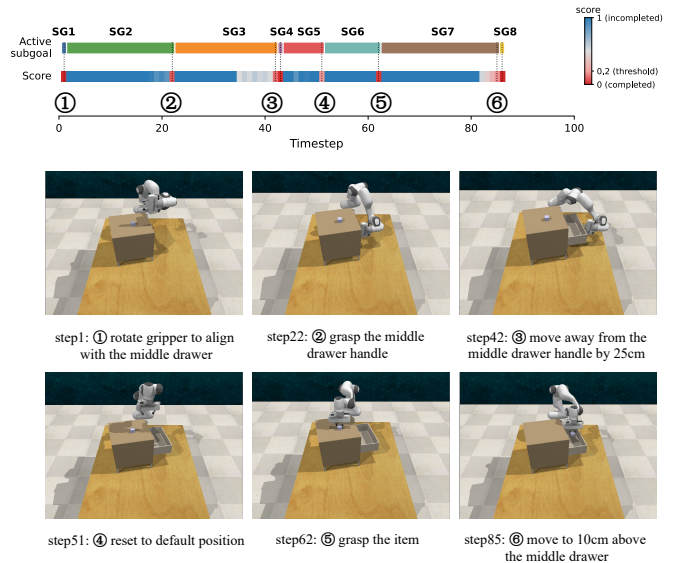


Fig. 5. Predicted subgoal completion scores for a representative successful trajectory of **ItemInDrawer**. The upper row shows the active subgoal over time, and the lower row shows the predicted completion score for the current subgoal. Lower scores indicate higher confidence that the current subgoal has been completed. The predicted scores decrease around the transitions between execution stages, indicating that the subgoal completion predictor is temporally aligned with the progress of the long-horizon task.

D. Ablation Study

We evaluate two ablative versions of SADP in simulation: (i) SADP w/o subgoal conditioning, which retains the subgoal completion prediction head but conditions the diffusion policy only on the task description; and (ii) SADP w/ oracle completion signal, which replaces the predicted completion signals

TABLE III
TASK SUCCESS RATES (%) FOR ABLATIONS OF SUBGOAL CONDITIONING AND COMPLETION PREDICTION IN SIMULATION.

Model	PutRubbish InBin	SlideBlock ToTarget	MeatOff Grill	Open Drawer	Close Drawer	PutItem InDrawer	Average
Ours(w/o subtask conditioning)	86.6 \pm 3.33	71.7 \pm 4.41	71.1 \pm 2.55	56.1 \pm 5.36	83.3 \pm 10.00	45.6 \pm 5.86	69.1
Ours(w/ oracle completion signal)	92.8 \pm 0.96	86.7 \pm 5.00	81.7 \pm 6.01	81.7 \pm 1.67	93.3 \pm 1.67	86.7 \pm 4.41	87.1
Ours	92.2 \pm 2.55	85.6 \pm 7.52	78.9 \pm 7.88	75.0 \pm 5.00	93.9 \pm 4.82	71.1 \pm 5.36	82.8

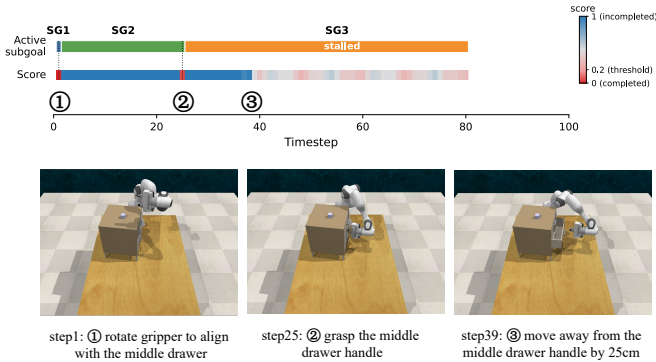


Fig. 6. Predicted subgoal completion scores for a representative failed trajectory of **ItemInDrawer**. The robot successfully completes the initial subgoals for aligning with and grasping the drawer handle, but the execution stalls during the drawer-opening subgoal. Because the gripper disengages from the handle during the opening motion, the completion of the third subgoal is not detected, and the active subgoal remains unchanged. This example illustrates how the predicted subgoal-level signal can help identify the stage at which the policy becomes stuck.

with ground-truth completion signals during execution. The results are summarized in Table III.

Removing subgoal conditioning leads to a substantial drop in task success rate, resulting in performance worse than the task-conditioned baseline TARAD. We attribute this degradation to a structural mismatch: the model is still trained to predict subgoal completion, but the action-generation branch receives only the task-level instruction. Consequently, the shared representation is encouraged to encode subgoal progression that cannot be directly exploited by the action-generation branch, which weakens action learning and reduces robustness in long-horizon execution. In contrast, using ground-truth completion signals improves success rates on long-horizon tasks. This result shows that accurate subgoal transition information is important for coordinating execution across multiple stages.

V. DISCUSSION

The results indicate that subgoal awareness is especially beneficial for long-horizon manipulation tasks with sequential dependencies. By conditioning the policy on the current natural-language subgoal, SADP maintains better temporal consistency than task-level policies and reduces failure accumulation across interaction stages. Importantly, this structure does not sacrifice task performance for transparency; instead, SADP achieves higher task success rates than strong task-conditioned baselines while exposing the active subgoal during execution. This transparency is supported by the data-generation process, where the same language-described sub-

goals are used as intermediate commands for foundation-model-based demonstration generation. Since only successful executions are retained, the subgoals are grounded in executable robot behavior.

The completion prediction head provides a simple mechanism for subgoal transitions. When the current subgoal is predicted as incomplete, the policy can continue or retry the same subgoal instead of prematurely executing subsequent actions. However, completion prediction is also a major source of failure. Different subgoals occupy different numbers of timesteps in the collected demonstrations, and short-duration subgoals provide fewer training samples for learning reliable completion boundaries. Consequently, the policy may skip an essential subgoal when completion is overestimated, or repeat an already completed subgoal when completion is underestimated. Consistent with this analysis, replacing the predicted completion signal with an oracle binary completion label improves performance, confirming the importance of reliable subgoal transition estimation.

Moreover, removing subgoal conditioning substantially degrades performance, suggesting that subgoal awareness should be integrated into action generation itself, rather than added only as an auxiliary explanation signal. Future work will focus on improving progress estimation, for example by predicting continuous task progress instead of relying only on binary completion prediction.

VI. CONCLUSIONS

In this work, we proposed SADP, a subgoal-aware diffusion policy trained from demonstrations automatically generated by foundation models. By decomposing long-horizon instructions into ordered natural-language subgoals and executing them sequentially, SADP eliminates the need for manual annotation for subgoal descriptions and completion signals. Through the integration of subgoal conditioning and a completion prediction head, SADP embeds human-interpretable subgoal structure directly into the diffusion-based action generation process.

Experimental results in simulation and real-robot settings demonstrate that SADP achieves strong performance in long-horizon manipulation tasks while providing subgoal-level execution signals for monitoring progress and diagnosing failures. The performance gains obtained with accurate completion signals further indicate that reliable subgoal transition estimation is important for long-horizon execution. These results show that interpretable subgoal structure and high task performance can coexist when interpretability is built directly into the

policy, offering a scalable pathway toward explainable autonomous robots capable of managing complex, long-horizon manipulation tasks.

REFERENCES

- [1] S. Wachter, B. Mittelstadt, and L. Floridi, “Transparent, explainable, and accountable ai for robotics,” *Science robotics*, vol. 2, no. 6, p. eaan6080, 2017.
- [2] O. Kroemer, S. Niekum, and G. Konidaris, “A review of robot learning for manipulation: Challenges, representations, and algorithms,” *Journal of machine learning research*, vol. 22, no. 30, pp. 1–82, 2021.
- [3] A. Correia and L. A. Alexandre, “A survey of demonstration learning,” *Robotics and Autonomous Systems*, vol. 182, p. 104812, 2024.
- [4] M. Hutsebaut-Buysse, K. Mets, and S. Latré, “Hierarchical reinforcement learning: A survey and open research challenges,” *Machine Learning and Knowledge Extraction*, vol. 4, no. 1, pp. 172–221, 2022.
- [5] M. Mersha, K. Lam, J. Wood, A. K. Alshami, and J. Kalita, “Explainable artificial intelligence: A survey of needs, techniques, applications, and future direction,” *Neurocomputing*, vol. 599, p. 128111, 2024.
- [6] W. Huang, C. Wang, R. Zhang, Y. Li, J. Wu, and L. Fei-Fei, “Voxposer: Composable 3d value maps for robotic manipulation with language models,” in *Conference on Robot Learning*. PMLR, 2023, pp. 540–562.
- [7] H. Ha, P. Florence, and S. Song, “Scaling up and distilling down: Language-guided robot skill acquisition,” in *Conference on Robot Learning*. PMLR, 2023, pp. 3766–3777.
- [8] S. Hu, T. Nagai, and T. Horii, “Tarad: Task-aware robot affordance-centric diffusion policy learned from llm-generated demonstrations,” *IEEE Robotics and Automation Letters*, 2025.
- [9] S. James, Z. Ma, D. R. Arrojo, and A. J. Davison, “Rlbench: The robot learning benchmark & learning environment,” *IEEE Robotics and Automation Letters*, vol. 5, no. 2, pp. 3019–3026, 2020.
- [10] C. Rudin, “Stop explaining black box machine learning models for high stakes decisions and use interpretable models instead,” *Nature machine intelligence*, vol. 1, no. 5, pp. 206–215, 2019.
- [11] T. Miller, “Explanation in artificial intelligence: Insights from the social sciences,” *Artificial intelligence*, vol. 267, pp. 1–38, 2019.
- [12] S. Anjomshoae, A. Najjar, D. Calvaresi, and K. Främling, “Explainable agents and robots: Results from a systematic literature review,” in *18th International Conference on Autonomous Agents and Multiagent Systems (AAMAS 2019)*, Montreal, Canada, May 13–17, 2019. International Foundation for Autonomous Agents and Multiagent Systems, 2019, pp. 1078–1088.
- [13] T. Sakai and T. Nagai, “Explainable autonomous robots: A survey and perspective,” *Advanced Robotics*, vol. 36, no. 5–6, pp. 219–238, 2022.
- [14] B. Hayes and J. A. Shah, “Improving robot controller transparency through autonomous policy explanation,” in *Proceedings of the 2017 ACM/IEEE international conference on human-robot interaction*, 2017, pp. 303–312.
- [15] M. Edmonds, F. Gao, H. Liu, X. Xie, S. Qi, B. Rothrock, Y. Zhu, Y. N. Wu, H. Lu, and S.-C. Zhu, “A tale of two explanations: Enhancing human trust by explaining robot behavior,” *Science Robotics*, vol. 4, no. 37, p. eaay4663, 2019.
- [16] S. Hu and T. Nagai, “Explainable autonomous robots in continuous state space based on graph-structured world model,” *Advanced Robotics*, pp. 1–17, 2023.
- [17] S. Hu, T. Horii, and T. Nagai, “Adaptive and transparent decision-making in autonomous robots through graph-structured world models,” *Advanced Robotics*, vol. 38, no. 22, pp. 1579–1599, 2024.
- [18] O. Nachum, S. S. Gu, H. Lee, and S. Levine, “Data-efficient hierarchical reinforcement learning,” *Advances in neural information processing systems*, vol. 31, 2018.
- [19] J. Li, C. Tang, M. Tomizuka, and W. Zhan, “Hierarchical planning through goal-conditioned offline reinforcement learning,” *IEEE Robotics and Automation Letters*, vol. 7, no. 4, pp. 10216–10223, 2022.
- [20] W. Li, X. Wang, B. Jin, and H. Zha, “Hierarchical diffusion for offline decision making,” in *International Conference on Machine Learning*. PMLR, 2023, pp. 20035–20064.
- [21] R. Yang, Z. An, L. Zhou, and Y. Feng, “Seqvla: Sequential task execution for long-horizon manipulation with completion-aware vision-language-action model,” *arXiv preprint arXiv:2509.14138*, 2025.
- [22] C. Chi, Z. Xu, S. Feng, E. Cousineau, Y. Du, B. Burchfiel, R. Tedrake, and S. Song, “Diffusion policy: Visuomotor policy learning via action diffusion,” *The International Journal of Robotics Research*, 10 2024.
- [23] Y. Ze, G. Zhang, K. Zhang, C. Hu, M. Wang, and H. Xu, “3d diffusion policy: Generalizable visuomotor policy learning via simple 3d representations,” in *Proceedings of Robotics: Science and Systems (RSS)*, 2024.
- [24] T.-W. Ke, N. Gkanatsios, and K. Fragkiadaki, “3d diffuser actor: Policy diffusion with 3d scene representations,” in *Conference on Robot Learning*. PMLR, 2025, pp. 1949–1974.
- [25] A. Brohan, Y. Chebotar, C. Finn, K. Hausman, A. Herzog, D. Ho, J. Ibarz, A. Irpan, E. Jang, R. Julian, et al., “Do as i can, not as i say: Grounding language in robotic affordances,” in *Conference on robot learning*. PMLR, 2023, pp. 287–318.
- [26] K. Lin, C. Agia, T. Migimatsu, M. Pavone, and J. Bohg, “Text2motion: From natural language instructions to feasible plans,” *Autonomous Robots*, vol. 47, no. 8, pp. 1345–1365, 2023.
- [27] W. Huang, P. Abbeel, D. Pathak, and I. Mordatch, “Language models as zero-shot planners: Extracting actionable knowledge for embodied agents,” in *International conference on machine learning*. PMLR, 2022, pp. 9118–9147.
- [28] S. Liu, Z. Zeng, T. Ren, F. Li, H. Zhang, J. Yang, Q. Jiang, C. Li, J. Yang, H. Su, et al., “Grounding dino: Marrying dino with grounded pre-training for open-set object detection,” in *European Conference on Computer Vision*. Springer, 2024, pp. 38–55.
- [29] N. Ravi, V. Gabeur, Y.-T. Hu, R. Hu, C. Ryali, T. Ma, H. Khedr, R. Rüdle, C. Rolland, L. Gustafson, et al., “Sam 2: Segment anything in images and videos,” in *The Thirteenth International Conference on Learning Representations*, 2025.
- [30] H. Huang, F. Lin, Y. Hu, S. Wang, and Y. Gao, “Copa: General robotic manipulation through spatial constraints of parts with foundation models,” in *2024 IEEE/RSJ International Conference on Intelligent Robots and Systems (IROS)*. IEEE, 2024, pp. 9488–9495.
- [31] Y. Jin, D. Li, A. Yong, J. Shi, P. Hao, F. Sun, J. Zhang, and B. Fang, “Robotgpt: Robot manipulation learning from chatgpt,” *IEEE Robotics and Automation Letters*, vol. 9, no. 3, pp. 2543–2550, 2024.
- [32] P. Hua, M. Liu, A. Macaluso, Y. Lin, W. Zhang, H. Xu, and L. Wang, “Gensim2: Scaling robot data generation with multi-modal and reasoning llms,” in *Conference on Robot Learning*. PMLR, 2025, pp. 5030–5066.
- [33] M. J. Kim, K. Pertsch, S. Karamcheti, T. Xiao, A. Balakrishna, S. Nair, R. Rafailov, E. P. Foster, P. R. Sanketi, Q. Vuong, et al., “Openvla: An open-source vision-language-action model,” in *Conference on Robot Learning*. PMLR, 2025, pp. 2679–2713.
- [34] K. Black, N. Brown, D. Driess, A. Esmail, M. Equi, C. Finn, N. Fusai, L. Groom, K. Hausman, B. Ichter, et al., “ π_0 : a vision-language-action flow model for general robot control,” *arXiv preprint arXiv:2410.24164*, 2024.
- [35] K. Black, N. Brown, J. Darpinian, K. Dhabalia, D. Driess, A. Esmail, M. R. Equi, C. Finn, N. Fusai, M. Y. Galliker, D. Ghosh, L. Groom, K. Hausman, B. Ichter, S. Jakubczak, T. Jones, L. Ke, D. LeBlanc, S. Levine, A. Li-Bell, M. Muthukuri, S. Nair, K. Pertsch, A. Z. Ren, L. X. Shi, L. Smith, J. T. Springenberg, K. Stachowicz, J. Tanner, Q. Vuong, H. Walke, A. Walling, H. Wang, L. Yu, and U. Zhilinsky, “ $\pi_{0.5}$: a vision-language-action model with open-world generalization,” in *Proceedings of The 9th Conference on Robot Learning*, ser. Proceedings of Machine Learning Research, J. Lim, S. Song, and H.-W. Park, Eds., vol. 305. PMLR, 27–30 Sep 2025, pp. 17–40.
- [36] Q. Zhao, Y. Lu, M. J. Kim, Z. Fu, Z. Zhang, Y. Wu, Z. Li, Q. Ma, S. Han, C. Finn, et al., “Cot-vla: Visual chain-of-thought reasoning for vision-language-action models,” in *Proceedings of the Computer Vision and Pattern Recognition Conference*, 2025, pp. 1702–1713.
- [37] A. Radford, J. W. Kim, C. Hallacy, A. Ramesh, G. Goh, S. Agarwal, G. Sastry, A. Askell, P. Mishkin, J. Clark, et al., “Learning transferable visual models from natural language supervision,” in *International conference on machine learning*. PMLR, 2021, pp. 8748–8763.
- [38] E. Perez, F. Strub, H. De Vries, V. Dumoulin, and A. Courville, “Film: Visual reasoning with a general conditioning layer,” in *Proceedings of the AAAI conference on artificial intelligence*, vol. 32, no. 1, 2018, pp. 3942–3951.
- [39] T.-Y. Lin, P. Goyal, R. Girshick, K. He, and P. Dollár, “Focal loss for dense object detection,” in *Proceedings of the IEEE international conference on computer vision*, 2017, pp. 2980–2988.
- [40] J. Achiam, S. Adler, S. Agarwal, L. Ahmad, I. Akkaya, F. L. Aleman, D. Almeida, J. Altenschmidt, S. Altman, S. Anadkat, et al., “Gpt-4 technical report,” *arXiv preprint arXiv:2303.08774*, 2023.